International Journal of Information, Control and Computer Sciences
ISSN: 2517-9942
Vol:5, No:8, 2011

Nonlinear Optimal Line-Of-Sight Stabilization with Fuzzy Gain-Scheduling

A. Puras Trueba, J. R. Llata García

***Abstract*—**A nonlinear optimal controller with a fuzzy gain scheduler has been designed and applied to a Line-Of-Sight (LOS) stabilization system. Use of Linear Quadratic Regulator (LQR) theory is an optimal and simple manner of solving many control engineering problems. However, this method cannot be utilized directly for multigimbal LOS systems since they are nonlinear in nature. To adapt LQ controllers to nonlinear systems at least a linearization of the model plant is required. When the linearized model is only valid within the vicinity of an operating point a gain scheduler is required. Therefore, a Takagi-Sugeno Fuzzy Inference System gain scheduler has been implemented, which keeps the asymptotic stability performance provided by the optimal feedback gain approach. The simulation results illustrate that the proposed controller is capable of overcoming disturbances and maintaining a satisfactory tracking performance.

***Keywords*—**Fuzzy Gain-Scheduling, Gimbal, Line-Of-Sight Stabilization, LQR, Optimal Control

I. Introduction

LINE-OF-SIGHT (LOS) stabilization systems, also known as stabilized platforms, are used in a plurality of applications to point sensors, cameras, antennas, instruments or weapons. All these applications have in common the use of this kind of system vehicle onboard. Vehicles used in such applications are ground vehicles, airplanes, helicopters, Unmanned Air Vehicles (UAVs), and even space satellites [3]. LOS stabilization systems possess the ability to maintain the LOS of a sensor or instrument when it is subjected to external disturbances caused by the carrier vehicle motion. One of the most demanding LOS stabilization system applications are electro-optical turrets, which have an optical sensor package payload consisting of CCD and/or IR camera, laser telemeter, etc. They can be employed in surveillance, target detection and tracking in border control, search and rescue or critical infrastructure security. The number of axes required by the system depends on the application requirements and it normally ranges from 2 to 5.

Electro-optical turrets can be found under different electromechanical configurations depending on the application. One of the most typical configurations consists of a combined structure of rotary actuators. Each rotary axis is known as gimbal. Although the requirements of such systems are imposed by the application, all of them follow the same objective, to hold or control the LOS of one object relative to another or to the inertial space. Moreover, they make use of inertial sensors such as accelerometers and gyroscopes, in most cases aided by one or several GPS receivers, to measure line of sight attitude changes and vehicle position in global coordinates.

Multigimbal electromechanical systems represent a complex nonlinear multivariable problem. Some factors, such as the mechanical resonance, the random drift of inertial sensors or the change of electric parameters among others, make the modeling of this kind of system difficult. Additionally, high dynamic operation imposed by some kinds of vehicles causes the coupling effect between axes to influence greatly the system performance, making impossible the use of decentralized control architectures. During the last decade, several controller design methods have been proposed for the stabilization of platforms, however, most of them are complex and difficult to implement in practice, and therefore, PID controllers keep being widely used in this kind of application.

In this work a nonlinear optimal control scheme of a LOS stabilization system by means of Linear Quadratic Regulators (LQR) and Fuzzy Gain Scheduler (FGS) is presented. During last decade, LQR theory has been widely used in many applications. Firstly, it can provide optimal controllers in terms of a cost function minimization. Moreover, LQR achieves a robust performance against model parameter uncertainties and disturbances [1], [2], [8]. In [7] a linear controller for the stabilization of a two-axis gimbal based on LQG/LTR was presented. A typical control design strategy employed to adapt LQ controllers to nonlinear system is Gain-Scheduling. However, this approach does not guarantee the overall stability of the controlled system under all possible situations when the system behavior is strongly nonlinear. To try to overcome this approximation problem the use of fuzzy systems has been investigated by many researchers [5], [11], and has been shown to perform well in terms of robustness and simplicity.

The idea of designing an adaptive controller LQR/FGS follows the implementation of an affordable controller capable of compensating model uncertainties, with proper transient response and stabilization performance. The proposed controller has been tested in simulations with real data in a two-gimbal, four Degrees-Of-Freedom (DOF) LOS stabilization system.

II. LOS Stabilization System Architecture

The LOS stabilization system architecture used in this paper is made up of two gimbals, one is considered as the inner gimbal while the other one is the outer. Each gimbal provides two DOF (Pan and Tilt). Figure 1 shows a schematic diagram of the system.

A. Puras Trueba is with the Aerospace Unit, Fundación Centro Tecnológico de Componentes, Cantabria, Santander, 39011 SPAIN (phone: +34-942-766976; fax: +34-942-766984; e-mail: apuras@ctcomponentes.com).
J. R. Llata García is with the Electronics Technology, Systems and Automation Engineering Department, University of Cantabria, Santander, 39005 SPAIN (e-mail: llata@teisa.unican.es).

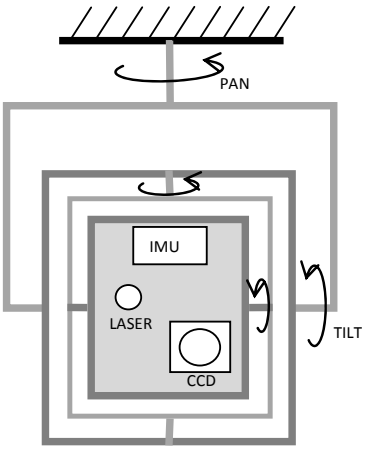

Fig. 1 LOS stabilization system architecture schematic diagram

The two outer gimbal axes are actuated by dc motors. The inner gimbal has attached to it the system payload (optical sensors and the inertial measurement unit, IMU) and it is mounted onto the outer gimbal. Its axes have a very limited range of angular movement because the inner gimbal is devoted to prevent sensor performance degradation caused by high frequency rotational vibrations. A magnet actuator provides the centering force to keep inner and outer axes aligned.

A. Forward Kinematics

To define the forward kinematics of the system the Denavit-Hartenberg convention has been used. The related parameters can be seen in Table 1.

TABLE I
DENAVIT-HARTENBERG PARAMETERS

Joint i	α_i [rad]	a_i [m]	θ_i [rad]	d_i [m]	R/P
1	–Π/2	0	θ_1	0	R
2	Π/2	0	θ_2	0	R
3	–Π/2	0	θ_3	0	R
4	Π/2	0	θ_4	0	R

$$T_0^4 = \begin{bmatrix} -\theta_3 s\theta_1 + c\theta_1(c\theta_2 - \theta_4 s\theta_2) & -\theta_3 c\theta_1 c\theta 2 - s\theta_1 \\ \theta_3 c\theta_1 + s\theta_1(c\theta_2 - \theta_4 s\theta_2) & c\theta_1 - \theta_3 c\theta_2 s\theta_1 \\ -\theta_4 c\theta_2 - s\theta_2 & \theta_3 s\theta_2 \\ 0 & 0 \end{bmatrix} \quad (1)$$

$$\begin{bmatrix} -\theta_3\theta_4 s\theta_1 + c\theta_1(\theta_4 c\theta_2 + s\theta_2) & 0 \\ \theta_3\theta_4 s\theta_1 + s\theta_1(\theta_4 c\theta_2 + s\theta_2) & 0 \\ c\theta_2 - \theta_4 s\theta_2 & 0 \\ 0 & 1 \end{bmatrix}$$

The homogenous transformation from the base of the system to the sensors coordinate frame is defined by the matrix T_0^4.

As the joint coordinates angles θ_3 and θ_4 in (1) are small, $s\theta_{3,4}$ has been approximated by $\theta_{3,4}$ and $c\theta_{3,4}$ by 1.

B. Differential Kinematics

Differential kinematics is used to find the relationship between the joint velocities and the end-effector linear and angular velocities. This relationship depends on the system geometry and it is expressed by the nonlinear matrix known as Jacobian,

$$v = J(q)\dot{q} \quad (2)$$

where v represents the end-effector velocity, q is the joint velocities vector, and $J(q)$ is the Jacobian.

In a generic multigimbal system all joints are rotations. Then the Jacobian can be expressed as

$$J_i = \begin{bmatrix} J_{vi} \\ J_{wi} \end{bmatrix} = \begin{bmatrix} z_{i-1} \times (p - p_{i-1}) \\ z_{i-1} \end{bmatrix}; \quad J = \begin{bmatrix} J_1 & \dots & J_n \end{bmatrix} \quad (3)$$

where p represents the end-effector position and z_i is obtained with the following expression:

$$z_i = R_0^i r_z \quad (4)$$

In (4) the vector $r_z = \begin{bmatrix} 0 & 0 & 1 \end{bmatrix}^T$ represents the rotation axis and R_0^i the rotation matrix from the base to the joint i.

The Jacobian for the presented architecture is:

$$J_w = \begin{bmatrix} J_{w1} & J_{w2} & J_{w3} & J_{w4} \end{bmatrix} \quad (5)$$

$$J_{w1} = \begin{bmatrix} 0 & 0 & 0 & 0 \\ 0 & 0 & 0 & 0 \\ 1 & 0 & 0 & 0 \end{bmatrix} \quad (5.1)$$

$$J_{w1} = \begin{bmatrix} 0 & -s\theta_1 & 0 & 0 \\ 0 & c\theta_1 & 0 & 0 \\ 1 & 0 & 0 & 0 \end{bmatrix} \quad (5.2)$$

$$J_{w1} = \begin{bmatrix} 0 & -s\theta_1 & c\theta_1 s\theta_2 & 0 \\ 0 & c\theta_1 & s\theta_1 s\theta_2 & 0 \\ 1 & 0 & 0 & 0 \end{bmatrix} \quad (5.3)$$

$$J_{w1} = \begin{bmatrix} 0 & -s\theta_1 & c\theta_1 s\theta_2 & -s\theta_1 - \theta_3 c\theta_1 c\theta_2 \\ 0 & c\theta_1 & s\theta_1 s\theta_2 & -c\theta_1 - \theta_3 c\theta_1 c\theta_2 \\ 1 & 0 & 0 & \theta_3 s\theta_2 \end{bmatrix} \quad (5.4)$$

III. DYNAMICS

The dynamics of the LOS stabilization system can be derived from the Euler-Lagrange formulation, which describes the behavior of a mechanical system subject to holonomic constraints.

The Lagrangian of a mechanical system is defined as the difference between the kinetic energy K and the potential energy V.

$$L = K - V \tag{6}$$

Before formulating the Euler-Lagrange equation, the expressions of the kinetic and potential energies will be derived.

A. Kinetic Energy

The kinetic energy of a rigid body can be considered as the addition of two energy terms, the translational energy, considering the mass of the body concentrated in its mass center, and the rotation energy.

The kinetic energy of a rigid body can be obtained from the following expression.

$$K = \frac{1}{2} m v^T v + \frac{1}{2} w^T I w \tag{7}$$

In (7), m is the total mass of the body, v and w are the translational and rotation velocities respectively, and I is the inertia tensor.

In our case, the kinetic energy of an n-joint robotic system can be expressed making use of the Jacobian defined in (5) in the following way.

$$\begin{bmatrix} v \\ w \end{bmatrix} = \begin{bmatrix} J_v \\ J_w \end{bmatrix} \dot{q} \tag{8}$$

Then, it can be derived from (7) and (8)

$$K = \frac{1}{2} \dot{q}^T \sum_{i=1}^{n} \left[m J_{vi}^T(q) J_{vi}(q) \right] \dot{q} + \\ + \frac{1}{2} \dot{q}^T \sum_{i=1}^{n} \left[J_{wi}^T(q) R_i(q) I_i R_i^T(q) J_{wi}(q) \right] \dot{q} \tag{9}$$

where $q = [q_1 \ \ldots \ q_n]^T$ is a vector which contains the joint variables.

Finally, a matrix expression for the kinetic energy can be obtained (10).

$$K = \frac{1}{2} \dot{q}^T D(q) \dot{q} \tag{10}$$

$D(q)$ is a symmetric positive definite matrix known as inertial matrix.

B. Potential Energy

The potential energy of a robot manipulator can be expressed by summing up all the potential energies of its elements. For an n-joint robot the potential energy is expressed in (11).

$$V = \sum_{i=1}^{n} V_i \tag{11}$$

V_i represents the potential energy of the element i. If all the elements in the system are rigid, then the potential energy is caused exclusively by the gravity. In these circumstances the potential energy of each element can be expressed as

$$V_i = \int_{Bi} g^T r_i dm = g^T \int_{Bi} r_i dm = g^T r_{ci} m_i . \tag{12}$$

In (12) g is the gravity acceleration vector, r_i is the position vector of each particle with mass dm and r_{ci} is the position vector of the mass center for the element i.

As it can be seen, the potential energy will depend only on the angular joint coordinates, q.

C. Euler-Lagrange Equation

Once the expressions for the kinetic and potential energy have been obtained it is possible to rewrite the Lagrangian as follows.

$$L = K - V = \frac{1}{2} \sum_{i=1}^{n} \sum_{j=1}^{n} d_{ij}(q) \dot{q}_i \dot{q}_j - V(q) \tag{13}$$

The expression of the Euler-Lagrange equation is as follows

$$\frac{d}{dt} \frac{\partial L}{\partial \dot{\lambda}_i} - \frac{\partial L}{\partial \lambda_i} = F_i \tag{14}$$

Where F_i is the generalized force related to the generalized coordinate λ_i. In our case, the generalized coordinates can be chosen to be the angular joint coordinates.

$$[\lambda_1 \ \ldots \ \lambda_n]^T = [q_1 \ \ldots \ q_n]^T \tag{15}$$

Then, from (13), (14) and (15) the two terms of the Euler-Lagrange equation can be derived.

$$\frac{d}{dt} \frac{\partial L}{\partial \dot{q}_i} = \sum_j d_{ij}(q) \ddot{q}_j + \sum_{j=1}^{n} \sum_{k=1}^{n} \frac{\partial d_{ij}}{\partial d_k} \dot{q}_k \dot{q}_j \tag{16}$$

$$\frac{\partial L}{\partial \dot{q}_i} = \frac{1}{2} \sum_{j=1}^{n} \sum_{k=1}^{n} \frac{\partial y}{\partial x} \dot{q}_k \dot{q}_j - \frac{\partial V}{\partial q_i} \tag{17}$$

The mathematical process to reach the expression of the system dynamics shown in (18) can be found in [6].

$$\sum_j d_{ij}(q) \ddot{q}_j + \sum_{j=1}^{n} \sum_{k=1}^{n} c_{ijk}(q) \dot{q}_k \dot{q}_j + g_i(q) = \tau_i \tag{18}$$

The c_{ijk} terms are known as the Christoffel symbols

$$c_{ijk} = \frac{\partial d_{ij}}{\partial q_k} - \frac{1}{2} \frac{\partial d_{jk}}{\partial q_i} \tag{19}$$

and $g_i(q)$ is:

$$g_i(q) = \frac{\partial V}{\partial q_i}. \quad (20)$$

Matrix equation (21) shows the dynamical model of the system.

$$D(q)\ddot{q} + C(q,\dot{q})\dot{q} + g(q) = \tau \quad (21)$$

In (21) τ is the torque.

Finally, the effects of non conservative forces can be added to the model. One of the main contributions to these forces are those caused by the static and viscous friction. The expression of the total torque considering the friction effects is as follows:

$$\tau = \tau_a - F_v\dot{q} - F_s\dot{q} \quad (22)$$

D.Passive Actuators

While the outer gimbal is actuated by dc motors, the inner gimbal posses a passive magnetic actuator, whose mission is to keep the inner gimbal centered with respect to the outer gimbal, damping high frequency rotational vibrations.

This kind of actuator can be modeled as a torsion spring where the potential energy can be expressed as follows,

$$V_s = \frac{1}{2}\alpha q_i^2; \quad i = 3,4 \quad (23)$$

Where α is the spring constant.

In [9] this kind of actuator is modeled by taking into account the additional effect of mechanical limits. Then, the potential energy is defined by (24), where β and nf are constant parameters.

$$V_s = \frac{1}{2}\alpha q_3^2 + \frac{1}{2}\alpha q_4^2 + \frac{1}{2}\frac{1}{\Pi+1}\beta(q_3^2 + q_4^2)^{nf+1} \quad (24)$$

E. Model Parameters

After formulating the dynamic equations of the system, the parameters of the system were introduced. Inertia tensors expressed in (25.1, 25.2, 25.3 and 25.4) are diagonal matrices.

Because of the geometric characteristics of the system the inertia tensor I_3 can be neglected.

$$I_1 = \begin{bmatrix} 0.561 & 0 & 0 \\ 0 & 1 & 0 \\ 0 & 0 & 2.247 \end{bmatrix} \left[kg/m^3 \right] \quad (25.1)$$

$$I_2 = \begin{bmatrix} 1.1 & 0 & 0 \\ 0 & 1 & 0 \\ 0 & 0 & 0.1 \end{bmatrix} \left[kg/m^3 \right] \quad (25.2)$$

$$I_3 = 0 \left[kg/m^3 \right] \quad (25.3)$$

$$I_4 = \begin{bmatrix} 0.111 & 0 & 0 \\ 0 & 0.01 & 0 \\ 0 & 0 & 0.01 \end{bmatrix} \left[kg/m^3 \right] \quad (25.4)$$

Since only two control inputs for two dc motors exist, the response of the system has been approximated by:

$$Pan = \theta_1 + \theta_3 \qquad Tilt = \theta_2 + \theta_4 \quad (26)$$

Moreover, the effect of the static friction F_s is supposed to be small enough to be neglected.

IV. Control System

The design of a controller capable of performing vehicle-mounted LOS stabilization must satisfy demanding operational specifications. Controller specifications must be established to provide the required isolation from carrier vehicle disturbances demanded by the payload. Usually, they are imposed by the resolution and the integration period of the optical sensors [3].

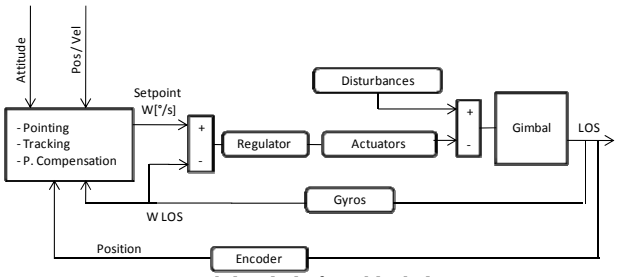

Fig. 2 Stabilized Platform block diagram

Two different control strategies exist to measure the attitude changes. These two approaches are known as *direct* and *indirect* LOS stabilization. The direct approach uses angular rate sensors (gyros) mounted together with the payload on the stabilized part of the system, to measure the LOS angular rates. On the other hand, in indirect LOS stabilization the gyros are mounted on the base of the system, measuring the vehicle angular rates. When the system is intended to perform LOS stabilization in high dynamic conditions, the direct approach is more appropriate. As the gyros are attached to the stabilized part of the system, angular rate measurements are less affected by nonlinearities and errors associated to the scale factor of the sensor, because the measured angular rates are close to zero [4]. The typical block diagram of an inertially stabilized platform control system is shown in figure 2. As can be seen, gyros are the sensors which measure the LOS angular rate.Stabilized platform control system design implies the implementation of two separated control loops, the pointing loop and the rate loop. The pointing loop generates rate commands to point the sensors towards the target, while the rate loop isolates the sensors from platform motion and

disturbances [3].The successful design of sophisticated controllers for LOS stabilization has been reported within the existing literature by several authors [6], [9], [10]. However, most of the related control designs imply an accurate modeling of the plant, and the implementation of complex controllers. Moreover, the model of the plant is commonly assumed to be time invariant. On the contrary, changes in the operation conditions such as temperature or humidity variations affect the parameters of the model. A kind of controller which combines robustness against model uncertainties and external disturbances and simplicity is the LQ. Moreover, it provides an optimal solution in terms of minimization of a designed cost function [1]. Although, this approach presents some disadvantages, (e.g. its formulation is only valid for linear systems, or the regulator tuning usually requires an iterative process to be carried out) is a good alternative to other advanced control strategies.

A. LQR Design

The main goal is to design a state feedback controller able to minimize the energy consumption. Within the development of this task a state-space model of the system is required. The expression (27) represents the state-space model of the system dynamics.

$$\dot{x} = \begin{bmatrix} \dot{x}_\theta \\ \dot{x}_w \end{bmatrix} = \begin{bmatrix} x_w \\ D(x_\theta)^{-1}(\tau_a - C(x_\theta, x_w)x_w - F_v x_w - K(x_\theta)x_\theta) \end{bmatrix} \quad (27)$$

Figure 3 shows the typical block diagram of a state-feedback LQR with setpoint input when states are fully observable.

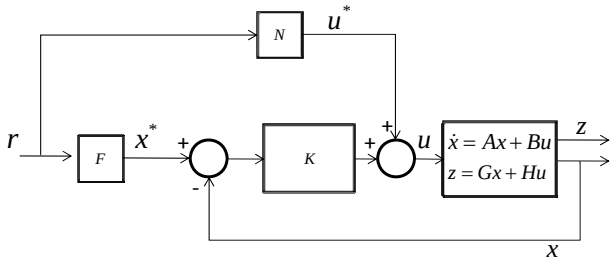

Fig. 3 State Feedback LQ controller with setpoint input

In figure 3, r and z represent the setpoint input and the output respectively. Vectors x^* and u^* are formed with the desired values of the state vector and the inputs of the plant. Both vectors can be determined from (28). The block K represents the optimal regulator, while F and N can be derived from the expressions in (29),

$$Ax^* + Bu^* = 0\,; \qquad r = Gx^* + Hu^* \quad (28)$$

and

$$x^* = Fr\,; \qquad u^* = Nr\,. \quad (29)$$

If the process has the same number of inputs and outputs, the system in (28) can be solved as shown in (30).

$$\begin{bmatrix} x^* \\ u^* \end{bmatrix} = \begin{bmatrix} A & B \\ G & H \end{bmatrix}^{-1} \begin{bmatrix} 0 \\ r \end{bmatrix} \quad (30)$$

The input of the plant generated by the optimal regulator K is presented in (31), and the associated cost function it minimizes is shown in (32).

$$u = K(x - x^*) + u^* = -Kx + (KF + N)r \quad (31)$$

$$J_{LQR} := \int_0^\infty \left(\|z(t)\|^2 + \rho \|u(t)\|^2 \right) dt \quad (32)$$

The term $z(t)$ in (32) corresponds to the energy of the controlled output and the term $u(t)$ to the energy of the control signal. Finally, ρ is a constant parameter used to balance the weight of both energy terms. Lower energy consumption in the controlled output implies higher energy consumption in the control signal and vice versa. Moreover, ρ can be used in loop-shaping to tune the controller in order to satisfy specific requirements in the frequency domain.The mathematic explanation to the presented optimization problem can be found in [2]. Equation (33) shows the solution expression for K, where P is the unique positive-definite solution of (34), known as the Algebraic Riccati Equation (ARE).

$$K = (H^T Q H + \rho R)^{-1}(B^T P + HQG) \quad (33)$$

$$A^T P + PA + G^T QG - (PB + G^T QH)(H^T QH + \rho R)^{-1} (B^T P + H^T QG) = 0 \quad (34)$$

Matrices Q and R can be designed according to the Bryson's rule. Then these matrices can be formed as follows (35.1 and 35.2).

$$Q_{ii} = \frac{1}{\max.\ acceptable\ value\ of\ z_i^2} \quad (35.1)$$

$$R_{jj} = \frac{1}{\max.\ acceptable\ value\ of\ u_j^2} \quad (35.2)$$

B. Linearization

LQR theory is developed according to the assumption of a Linear Time Invariant (LTI) plant. However, the multigimbal architecture of the LOS stabilization system, represented by the function f in (36) and presented in (27), is clearly non linear.

$$\dot{x} = f(x,u) \tag{36}$$

To apply the Gain-Scheduling control methodology to our system, the design of a linearization procedure is required. The linearization will be applied to the nonlinear system at a set of selected operating points. Then, the resulting linear models will be used to design the associated LQ controllers.

The local linearized model is represented in (37), where $x_l = x - x_0$ and $u_l = u - u_0$, being x_0 and u_0 the state and input vectors which define the operating point.

$$\dot{x}_l = Ax_l + Bu_l \tag{37}$$

Matrices A and B in (37) can be obtained applying partial derivatives to f at each operating point.

$$a_{ij} = \frac{\partial f_i}{\partial x_j}\bigg|_{x_0,u_0}; \qquad b_{ij} = \frac{\partial f_i}{\partial u_j}\bigg|_{x_0,u_0} \tag{38}$$

C. Fuzzy Gain-Scheduling

Gain-Scheduling is a control mechanism that enables the use of linear controllers in complex nonlinear systems. Since a nonlinear system can be approximated at given operating points by local linearization, the stable operation of linear controllers around these points is possible. A gain scheduler provides the continuation of use of the linear control scheme to all the possible operation points achieving the intended performance. However, classical Gain-Scheduling based on linear interpolation does not guarantee the overall stability of the system, because it is not able to model nonlinearities between two operation points. To overcome this problem FGS can be used, which can approximate the in-between regions in a more accurate way [11].

A FGS can be implemented as a Takagi-Sugeno fuzzy controller. If linearized models associated to the operating points s^i, $i = 1, 2, \ldots l$ are considered, the system can be approximated by the fuzzy rule base as

$$R^i: \; If \; s \; is \; F^i \; then \; x_l^i = A^i x_l^i + B^i u_l^i, \tag{39}$$

$$\text{with } i = 1, 2, \ldots l, \tag{40}$$

where R^i denotes the i^{th} fuzzy inference rule. Each fuzzy rule expresses the local dynamics by a linear system model. The optimal feedback controller for the linearized system is of the following form:

$$R^i: \; If \; s \; is \; F^i \; then \; u = K^i(x^i - x^{*i}) + u^{*i} \tag{41}$$

F^i is the fuzzy set of each rule, and μ_F^i is the associated fuzzy membership function. It can be interpreted as the grade of membership of s in F^i.

In order to achieve a more adaptable solution the fuzzy membership function can be chosen as

$$\mu_F^i(s) = \exp(-(s - s^i)^2 / 2\sigma_i^2), \tag{42}$$

where both the operating point s^i and σ_i can be tuned to get a robust and satisfactory performance. Fuzzy membership function parameters and the set of operating points can be optimally determined in an automatic fashion by using the evolutionary technique presented in [11].Finally, the FGS can be derived by considering an average weighting as follows

$$w^i = \frac{\mu_F^i(s)}{\sum_{i=1}^{l} \mu_F^i(s)} \tag{43}$$

$$\dot{x} = \frac{\sum_{i=1}^{l} \mu^i (A^i x_l^i + B^i u_l^i)}{\sum_{i=1}^{l} \mu^i(s)} = \sum_{i=1}^{l} w^i (A^i x_l^i + B^i u_l^i) \tag{44}$$

$$\dot{x} = \frac{\sum_{i=1}^{l} \mu^i (K^i(x^i - x^{*i}) + u^{*i})}{\sum_{i=1}^{l} \mu^i(s)} = \sum_{i=1}^{l} w^i (K^i(x^i - x^{*i}) + u^{*i}) \tag{45}$$

The effectiveness of the controller presented in (45) relies on the selected set of operating points and the tuning of both the LQ regulator and the fuzzy membership function parameters.

D. Nonlinear Optimal Controller

From the analysis of the dynamical model formulated in section 3 it can be deduced that joint coordinate θ_2 has the strongest influence on the nonlinear behavior of the system. Therefore, this joint coordinate has to be chosen as the input to the fuzzy system to be able to model the nonlinearities of the plant.By making use of simulations and after an iterative process, a set of four operating points were selected (θ_2 = 0, $\Pi/6$, $\Pi/3$, $\Pi/2$). At the same time, the related linearized models and their optimal LQ controllers were obtained. Figure 4 shows the simulation results for the stabilization error obtained in the Tilt angle considering two different sets of membership functions.

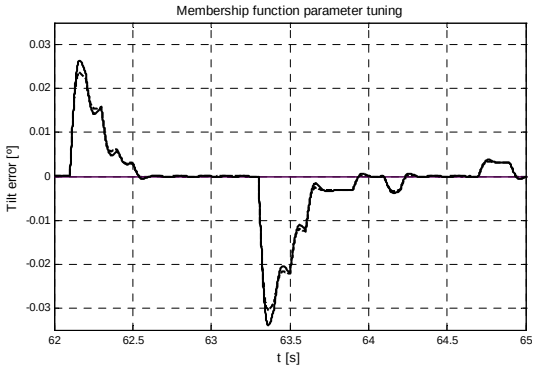

Fig. 4 Error in Tilt angle considering two different sets of membership functions.

The fuzzy membership functions defined after this process are shown in figure 5.

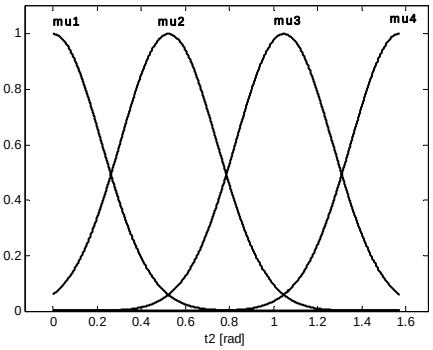

Fig. 5 Fuzzy membership functions

The parameter σ_i affects the overlap between the membership functions. It was adjusted to 0.22.

Matrices Q and R presented in (35) were defined as follows.

$$Q = \begin{bmatrix} 1/(2\Pi)^2 & 0 \\ 0 & 1/(0.5\Pi)^2 \end{bmatrix} \left\lfloor 1/rad^2 \right\rfloor \tag{46.1}$$

$$Q = \begin{bmatrix} 1/2^2 & 0 \\ 0 & 1/1.8^2 \end{bmatrix} \left\lfloor 1/(Nm)^2 \right\rfloor \tag{46.2}$$

Finally, in order to tune the transient response of the system, several parameterizations of the LQ controllers with different values for ρ were required. These controllers were also tested using simulations and finally ρ parameters were established.

In figures 6 and 7 can be seen how the ρ parameter influences the transient step response of the system. By reducing the value of ρ the response becomes faster and therefore the bandwidth of the system results increased. On the other hand the overshoot is slightly increased.

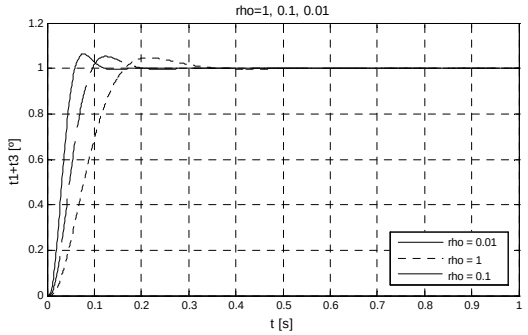

Fig. 6 Pan angle step response for different values of ρ

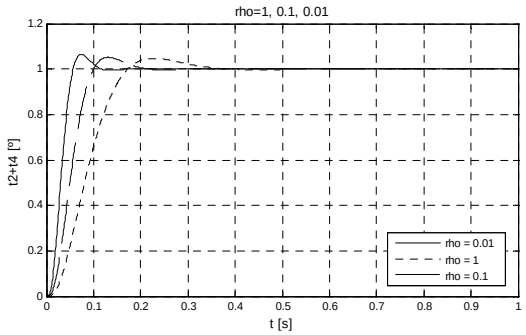

Figure 7: Tilt angle step response for different values of ρ

V. Simulations Results

In order to prove the stability and satisfactory performance of the designed controller, several simulations under real carrier vehicle disturbances were carried out. The applied attitude disturbances were obtained from measurements taken with an inertial navigation system (INS) mounted on a car, while travelling through urban areas. The INS was configured to provide 100 Hz data output rate. The LOS coordinates were determined to point at a far away target defined by its global coordinates. Therefore, the system aim was to stabilize the LOS to keep on tracking the mentioned static target.

Figure 8 shows the simulated system response for the Pan angle, while the car was going through two roundabouts.

For the same 125-second period of time, figure 9 shows the simulation results for the Tilt angle.

Figure 10 shows the stabilization error along the simulation where peaks of error can be seen. These peaks of error are due to abrupt changes in the heading angle estimated by the IMU, caused by internal Kalman Filter divergences under high accelerations. Figure 11 shows this effect in more detail.

Finally, figure 12 and 13 show the weighting values applied to the fuzzy membership functions to compute the interpolated controllers. In figure 13 weight variations can be observed during a shorter period of time when Tilt angle suffered a fast change.

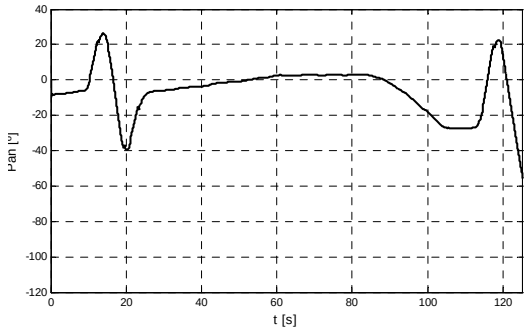

Fig. 8 System response for the Pan angle through two roundabouts

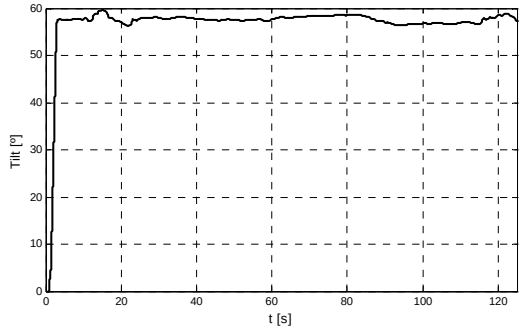

Fig. 9 System response for the Tilt angle through two roundabouts

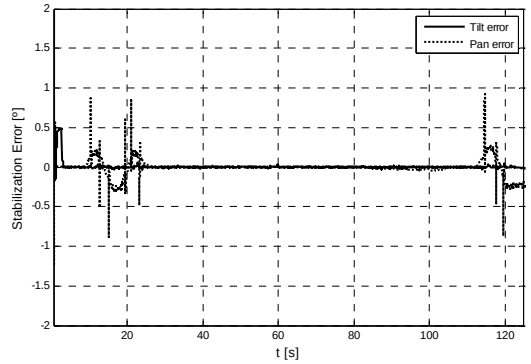

Fig. 10 Stabilization error (Pan and Tilt) obtained along the simulation.

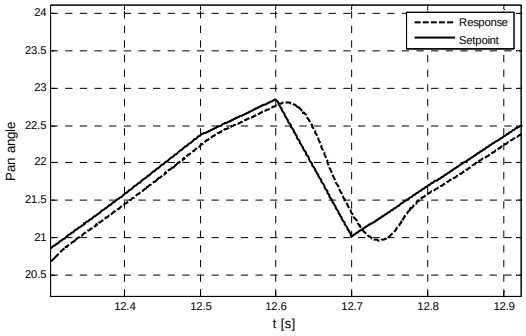

Fig. 11 Detail of the setpoint and response during an abrupt change in the heading angle provided by the IMU.

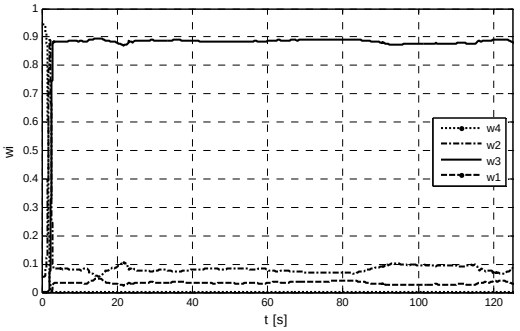

Fig. 12 Weighting values for the four fuzzy membership functions

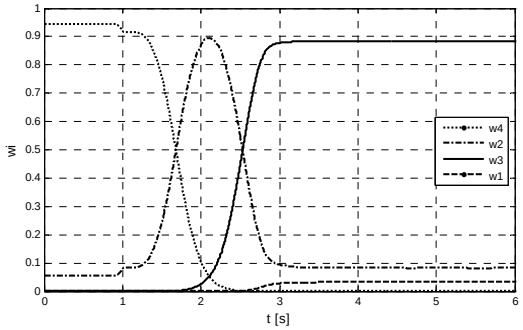

Fig. 13 Weighting values for the four fuzzy membership functions in greater detail

VI. Conclusions

A nonlinear optimal controller for LOS stabilization systems based on Linear Quadratic Regulators (LQR) and a Fuzzy Gain-Scheduling (FGS) has been designed. Firstly, the kinematic and dynamic models of a 2-gimbal 4-DOF LOS stabilization system were obtained. Then, the LQR design and the linearization procedures were presented. Furthermore, a FGS control methodology was designed which is able to improve the approximation between the operating points. In order to prove the stability and satisfactory performance of the designed controller, several simulations under real carrier vehicle attitude disturbances were carried out. The attitude disturbances were formed from measurements taken with an Inertial Navigation System mounted on a car, while travelling through urban areas. A static target defined by its global coordinates was employed, in such a way that the system aim was to stabilize the LOS. The obtained results prove the stability of the system under the imposed high dynamic conditions. Moreover, the controller provides a satisfactory dynamic response achieving admissible pointing errors during the performed simulations.

References

[1] B. D. O. Anderson, and J. B. Moore, Optimal Control Linear Quadratic Methods. Prentice Hall, 1990.
[2] J. P. Hespanha, "Lecture Notes on LQG/LQR controller design", 2005.
[3] J. M. Hilkert, "Inertially Stabilized Platform Technology", IEEE Control Systems Magazine, 2008.
[4] P. J. Kennedy, "Direct Versus Line of Sight (LOS) Stabilization", IEEE Transactions on Control Systems Technology, Vol. 11, No. 1, 2003.
[5] R. Palm and U. Rehfuess, "Fuzzy Controllers as Gain Scheduling Approximators", Fuzzy Sets and Systems, Vol. 85, 1997.
[6] L. Sciavicco and B. Siciliano, Modelling and control of robot manipulators, The McGraw-Hill Companies, Inc, 1996.
[7] K-J. Seong et Al., "The Stabilization Loop Design for a Two-Axis Gimbal System Using LQG/LTR Controller", SICE-ICASE International Joint Conference, Busan, Korea, 2006.
[8] S. Skogestad and I. Plostethwaite, Multivariable Feedback Control Analysis and Design, John Wiley & Sons, 2001, pp. 355–368.
[9] P. Skoglar, "Modeling and control of IR/EO-gimbal for UAV surveillance applications", Thesis, 2002.
[10] P. Wongkamchang and V. Sangveraphunsir, "Control of Inertial Stabilization Systems Using Robust Inverse Dynamics Control and Adaptive Control", Thammasat Int. J. Sc. Tech., Vol. 13, No. 2, 2008.
[11] B. Wu and X. Yu, "Evolutionary Design of Fuzzy Gain Scheduling Controllers", Proceedings of the Congress on Evolutionary Computation, 1999.